MTR090458

MITRE TECHNICAL REPORT

MITRE

Analysis of ANLE Compatibility with MSS Feeder Links

Dr. Izabela L. Gheorghisor
Dr. Yan-Shek Hoh
Dr. Alexe E. Leu

December 2009

CAASD

MTR090458

MITRE TECHNICAL REPORT

MITRE

Analysis of ANLE Compatibility with MSS Feeder Links

Dr. Izabela L. Gheorghisor
Dr. Yan-Shek Hoh
Dr. Alexe E. Leu

December 2009

Sponsor: Federal Aviation Administration
Dept. No.: F043
Project No.: 0210F902-AN
Outcome No.: 2
PBWP Reference: 2-1.A.1-1, "Analysis of ANLE Compatibility with Satellite Feeder Links"

For Release to all FAA
Approved for public release; distribution unlimited.

Abstract

The Federal Aviation Administration plans to use the 5091-5150 megahertz band for wireless broadband networks on airport surfaces. These are denoted as Airport Network and Location Equipment (ANLE) networks in our report. The same frequency band has also been allocated to non-geostationary mobile-satellite-service (MSS) feeder uplinks. This report presents an analysis of ANLE compatibility with MSS feeder uplinks. The results show that, given the system parameters defined in Sections 2 and 3 of this report, bandsharing is feasible between ANLE networks and MSS feeder uplinks.

Table of Contents

List of Figures

List of Tables

1 Introduction

The Airport Network and Location Equipment (ANLE) networks currently being planned by the Federal Aviation Administration (FAA) will support high-data-rate wireless broadband communications in an airport surface environment. The FAA is considering the use of the 5091-5150 megahertz (MHz) band for the implementation of such networks. The potential future use of the 5000-5030 MHz band is also being studied. ANLE networks are expected to use the Orthogonal Frequency-Division Multiple Access (OFDMA) implementation described in the Institute of Electrical and Electronics Engineers (IEEE) 802.16e standard documents [1], [2]. However, the 5091-5150 MHz band has also been allocated, on a co-primary basis, to non-geostationary (non-GSO) mobile-satellite-service (MSS) Earth-to-space feeder uplinks under footnote S5.444A in the International Allocation Tables and Resolution 114 of the 1995 World Radiocommunication Conference (WRC-95).

In 2005, the FAA spectrum office requested The MITRE Corporation's Center for Advanced Aviation System Development (CAASD) to investigate whether measures may be needed to protect the MSS feeder uplinks from potential cochannel radio frequency (RF) interference (RFI) due to ANLE transmissions. In that preliminary investigation, each airport was assumed to be employing a single ANLE base station transmitter using an omnidirectional antenna and operating in the Orthogonal Frequency-Division Multiplexing (OFDM) scheme. The findings of that study were documented in [3].

Since then, International Telecommunication Union (ITU) World Radiocommunication Conference 2007 (WRC-07) has developed a new MSS RFI criterion for stations of the aeronautical mobile (route) service (AM(R)S) limited to surface applications in the 5091-5150 MHz band. Since the 2005 analysis, MITRE/CAASD has also investigated various configurations suitable for ANLE operations [4].

To support the ATO-W/Spectrum work for upcoming ITU meetings regarding spectrum allocations for these systems, the FAA requested CAASD to update its 2005 analysis using the new information on the recently changed MSS-AM(R)S RFI criterion as well as updated ANLE parameters. The updated analysis considers interference effects from multiple ANLE base stations (BSs) at the same airport, evaluates interference to MSS satellite receivers from ANLE networks with sectorized BSs, and analyzes the effects of multiple simultaneous OFDMA transmissions. This report presents the results of the effort.

2 ANLE Characteristics

This section introduces the relevant features of the ANLE systems to be considered in the present analysis.

2.1 ANLE Description

As in [3], we identified 497 towered airports in the contiguous United States (CONUS) that are expected to be the primary candidates for ANLE system installations. Multiple BSs are used at a given airport [4] such that the radius of the coverage area for each BS could be kept below 2 km as recommended in [5]. The theoretical area covered by a given BS is a circle of radius r_0=1.73 km. A configuration considered for a typical airport of radius R_0=3 km (the area enclosed by the dashed circle) will use three BSs as shown in Figure 2-1.

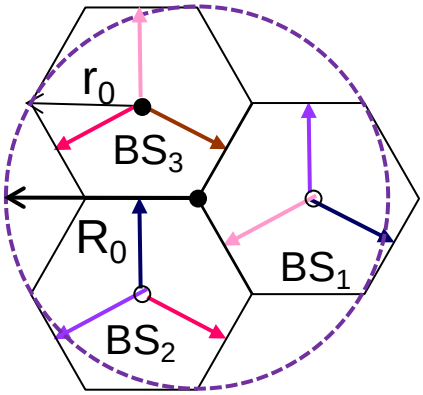

Figure 2-1. Typical Configuration with 10-MHz Channels and Sectoral Antennas

Three sectors are considered at each BS. The direction of each arrow signifies the direction of the main beam in each sector. There are areas within the 3-km circle where users would need to use repetition coding for data transmission and reception; so the physical layer data rates would be smaller for users in these areas. There are five channels (represented by different colors) assumed available per airport. Each channel bandwidth is 10 MHz. The reuse of the colors in this setup signifies the frequency reuse for the five 10-MHz channels among the various BS sectors. In the configuration shown in Figure 2-1 and assumed in the present investigation at each airport, two BS sectors with main beam azimuth angles 120º apart can use the same frequency channel for transmission.

2.2 ANLE Antenna Patterns for Base Stations and Subscriber Units

The antenna patterns for the ANLE system are based on the ITU Radiocommunication Sector (ITU-R) F.1336-2 recommendation [6]. Each BS is assumed to cover each of three 120° sectors with a sectoral transmitting antenna having a maximum gain (G_{max}) of 15 dBi.

The azimuth and elevation radiation patterns for such antennas are shown in Figure 2-2 and 2-3, respectively.

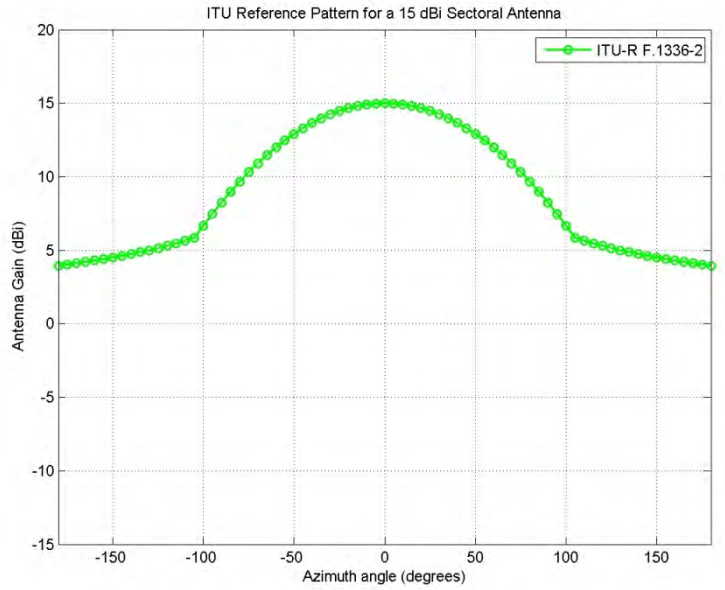

Figure 2-2. Azimuth Pattern for a Sectoral Antenna with G_{max} = 15 dBi

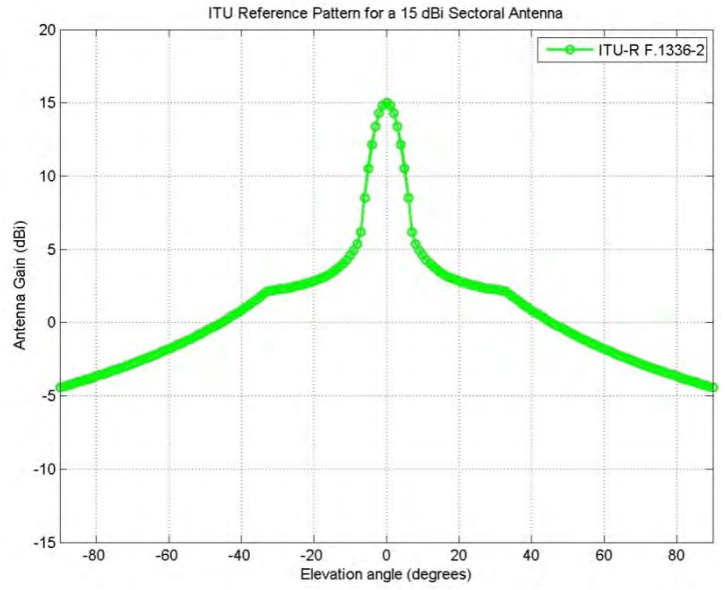

Figure 2-3. Elevation Pattern for a Sectoral Antenna with G_{max} = 15 dBi

An ANLE network user is denoted as a subscriber unit (SU). In the present analysis, it is assumed that the antenna pattern of an SU is omnidirectional in the azimuth plane with a maximum gain of 6 dBi. Figure 2-4 illustrates the elevation pattern as described in [6].

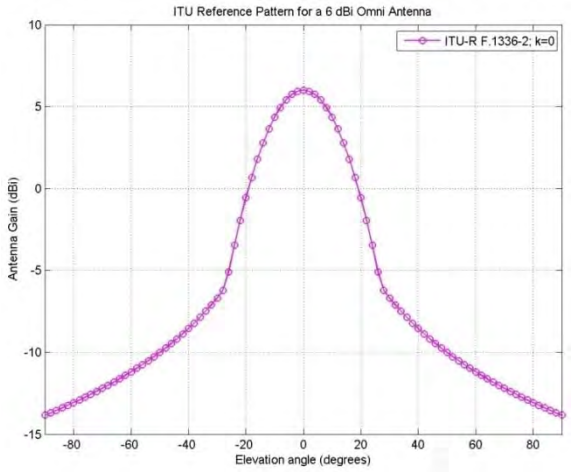

Figure 2-4. Elevation Pattern for an Omnidirectional Antenna with G_{max} = 6 dBi

2.3 ANLE Parameters Used in the Analysis

The ANLE transmitter power required to establish a 1.73-km direct link can be estimated on the basis of a set of nominal parameter values. A receiver sensitivity value of -92.36 dBm is used for the BS receivers, assuming a noise figure of 5 dB and an implementation loss of 2 dB. A receiver sensitivity value of -90.36 dBm is used for the SU receivers, assuming a noise figure of 7 dB and an implementation loss of 2 dB. These receiver sensitivity values are based on receiver characteristics described by the Worldwide Interoperability for Microwave Access (WiMAX) Forum in [7], [8], the methodology presented in [1], and the assumption of Quadrature Phase-Shift Keying (QPSK) ½ modulation and coding. It should also be noted that the methodology for evaluating receiver sensitivities described in the IEEE 802.16-2009 consolidated standard [9] is the same as the methodology described in the IEEE 802.16e document.

The path loss is a function of the path distance *d* in kilometers (km). For an ANLE system the propagation path loss is evaluated on the airport surface where the path loss characteristics could be different from the free-space path loss. The path loss exponent *n* and the characteristic distance d_{0km} estimated in [5] are used to characterize the environment. The path loss, in decibel (dB), is defined as:

$$L_{path}(d) = L_{free}(d_{0\,km}) + 10n\log_{10}(d / d_{0km}) \qquad (2\text{-}1)$$

where:

L_{free} = free-space path loss (dB),
d_{0km} = propagation distance (km) up to which path loss can be modeled using the free-space equation,
n = path loss exponent used beyond d_{0km}

and

$$L_{free}(d_{0\,km}) = 32.44 + 20\log_{10}(f_{MHz}) + 20\log_{10}(d_{0km}) \qquad (2\text{-}2)$$

with

f_{MHz} = operating frequency (MHz).

In [5], it was noted that the path loss value at distance d_{0km} based on measurements was about 3 dB higher than free-space path loss at that distance. In order to incorporate this finding into our analysis, the 3-dB difference is included into the system margin described below.

In the present analysis a fade margin of 11 dB, and a pilot power boosting factor of -0.46 dB for the forward link (FL) and 0 dB for the reverse link (RL), are used [1], [4]. Also included are a cable loss of 1 dB, and a system margin of 9 dB. An interference margin of 2 dB for the FL and 3 dB for the RL are considered as well [7]. The values used for the various margins need to be further validated by simulations and/or field tests (which are beyond the scope of the present study). In addition, we assume that each receiver employs two receiving antennas to achieve a receive diversity gain of 3 dB. The required ANLE transmitter power P_t, in dB referred to one milliwatt (dBm), is computed using the following expression:

$$P_t = R_{xs} + L_{path}(d) + L_{fm} + L_{im} + L_{sm} + L_c - G_t - G_r - G_{rx,div} - \zeta_{PB} \quad (2\text{-}3)$$

where:

R_{xs} = receiver sensitivity in dBm,
d = distance in km,
G_t = transmitter antenna gain in dB referred to lossless isotropic gain (dBi),
G_r = receive antenna gain in dBi,
$G_{rx,div}$ = receive diversity gain in dB,
L_{fm} = fade margin in dB,
L_{im} = interference margin in dB,
L_{sm} = system margin in dB,
L_c = cable loss in dB, and
ζ_{PB} = pilot power boosting factor in dB.

Table 2-1 summarizes the ANLE system parameters.

Table 2-1. ANLE System Parameters

Parameter	Value
BS Receiver Sensitivity $R_{xs,BS}$ (dBm)	-92.36
BS Antenna Gain $G_{BS,max}$ (dBi)	15
Cable Loss L_c (dB)	1
Pilot Power Boosting Factor ζ_{PB} (dB)	-0.46 (FL) 0 (RL)
Fade Margin L_{fm} (dB)	11
Interference Margin L_{im} (dB)	2 (FL) 3 (RL)
System Margin L_{sm} (dB)	9
Path-loss exponent n	2.3
Distance d_0 (km)	0.462
SU Antenna Gain G_{SU} (dBi)	6
RX Diversity Gain $G_{rx,div}$ (dB)	3
SU Receiver Sensitivity $R_{xs,SU}$ (dBm)	-90.36

The ANLE transmitter power levels required to establish a 1.73-km communications link in the system as determined using equation (2-3) are 22.3 dBm for BS and 20.9 dBm for SU.

For the present analysis, a worst-case setup is also assumed in which the duty cycle of ANLE transmissions is 100%, i.e., continuous transmission in all ANLE airports (either on the FL or RL). In a real-world situation, however, the duty cycle values are expected to be less than 100%. A 50% value was discussed in the prior ANLE-to-MSS compatibility study [3]. (It should be also noted that duty cycle values in the range of 1% to 15% were under consideration for sharing studies in the 5150-5250 MHz as mentioned in [3]). Detailed design studies will be needed to ascertain practical duty-cycle values for ANLE transmitters.

3 Satellite System Characteristics

The interference victim to be considered in the analysis is the low-earth-orbit (LEO) satellite system HIBLEO-4. This section outlines the features and technical parameters of the HIBLEO-4 satellite receiver.

The HIBLEO-4 satellite has a 109.9° field of view (FOV) covering approximately 9% of the Earth's surface. The height of the satellite orbit is 1414 km. Its receiving antenna gain in the FOV has a constant value of 4 dBi. Figure 3-1 illustrates the geometrical concept.

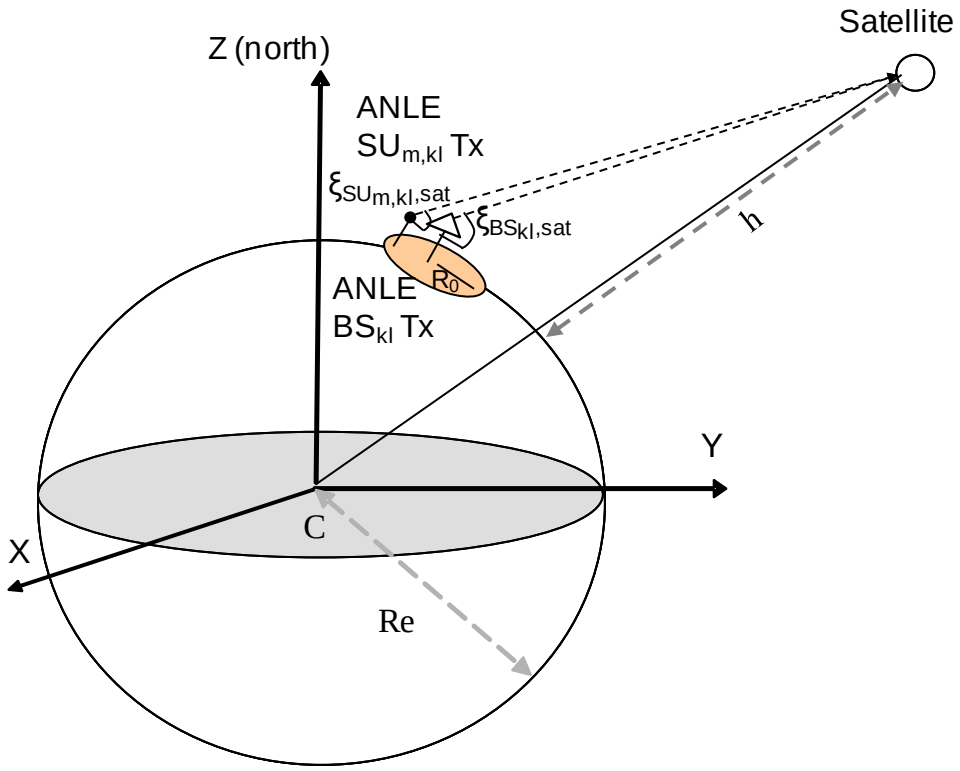

Legend
C: center of Earth
h: altitude of satellite above mean sea level (AMSL) (1414 km)
Tx: transmitter
BS_{kl}: sector l of base station k
$SU_{m,kl}$: m^{th} subscriber unit communicating with BS_{kl}
Re: Earth's radius (6378 km)
R_0: radius of ANLE coverage (3 km) ($R_0 << h$)
ξ: elevation angle

Figure 3-1. Illustration of Satellite Receiver and ANLE Transmitters

As in [3], we identified 497 towered airports in the contiguous United States (CONUS) that are expected to be the primary candidates for ANLE system installations. Figure 3-2 shows

(in light blue) the full set of "relevant" 2° x 2° latitude/longitude cells such that a satellite directly above the center of a given cell would be in view of at least one of the 497 towered CONUS airports (shown in dark blue in the figure).

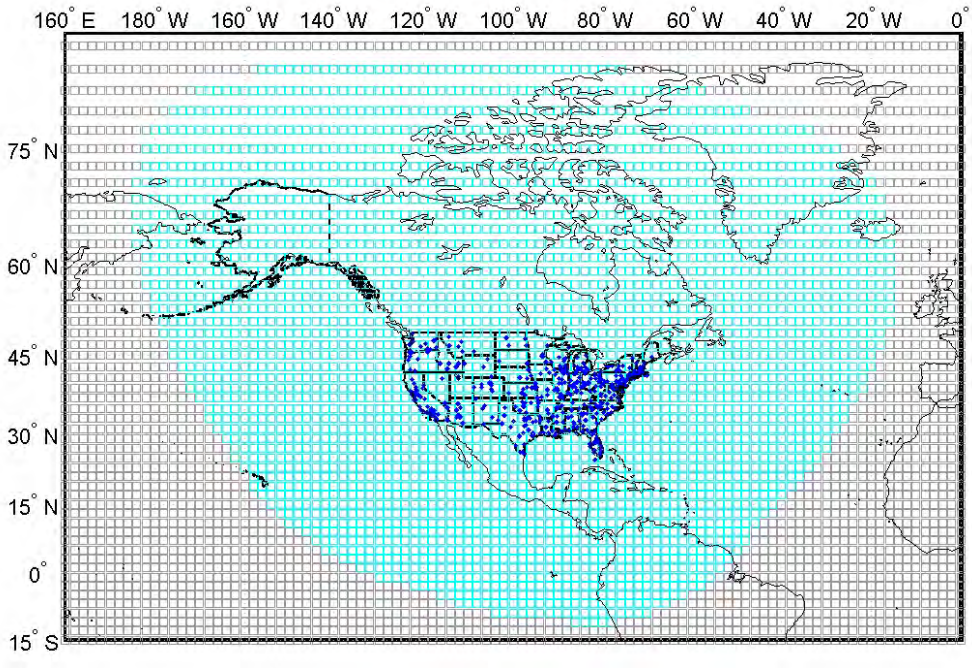

Figure 3-2. Relevant Cells for HIBLEO-4 Considered in Analysis

The 5091-5150 MHz band has been allocated, on a co-primary basis, to non-GSO MSS Earth-to-space feeder uplinks, aeronautical mobile telemetry (AMT), and AM(R)S including the aeronautical mobile service (AMS) limited to aeronautical security (AS). The aggregate power flux density (pfd) of these terrestrial services at the satellite receiver is limited to increasing the satellite receiver noise temperature (ΔT/T) by no more than 3%. Under Annex 1 to Resolution 418 of WRC-07, the RFI apportionment is 1% to AMT [10]. Thus the apportioned RFI allowance due to AM(R)S plus AS is limited to 2% of the satellite receiver thermal noise equivalent. As mentioned in ITU-R M.1827 recommendation [11], in order not to exceed a ΔT/T of 2%, stations of the AM(R)S and AS stations operating within the footprint of a single satellite should coordinate. In the present analysis, we will focus on ANLE implementations assuming that such coordination has been done.

In the following analysis, we adopt the interference criterion of a 2% increase of the satellite receiver's noise temperature. This criterion can be translated into an interference threshold, *H*, that must not be exceeded at the satellite receiver by the aggregation of power received from all transmitting ANLE devices in view of the victim receiver. The interference threshold, in dB referred to one watt (dBW), is determined according to the following expression:

$$H = 10\log_{10}(kBTC) \qquad (3\text{-}1)$$

where

k = Boltzmann's constant = 1.38×10^{-23} joules/K
B = bandwidth of the receiver (hertz)
T = noise temperature of the receiver (K), and
C = 2%.

Table 3-1 shows the values of key HIBLEO-4 parameters. The threshold value as determined using equation (3-1) is seen to be -157.3 dBW. Much of the data presented here can be found in [11], [12].

Table 3-1. Parameter Values Used in Satellite Interference Calculations

Parameter	HIBLEO-4
Satellite orbit altitude h (km)	1414
Satellite receiver noise temperature T (K)	550
Criterion C	2%
Interference threshold H (dBW)	-157.3
Polarization discrimination L_p (dB)	1
Feed loss L_{feed} (dB)	2.9
Satellite receiver bandwidth B (MHz)	1.23
Width of field of view (degrees)	109.9
Satellite receive antenna gain (dBi)	4
Satellite receiving antenna effective area (dBm^2)	-35.6
Earth radius (km)	6378

The bandwidth factor, B_f, is the ratio of the victim satellite receiver bandwidth (B_{sat}) to the interfering ANLE transmitter bandwidth (B_{ANLE}), if $B_{sat} < B_{ANLE}$; otherwise, $B_f = 1$ (i.e., 0 dB). It determines the amount of interfering power falling into the satellite receiver bandwidth. Recall that the channel bandwidth for ANLE is assumed to be 10 MHz. This value is larger than the receiver bandwidth of HIBLEO-4. Therefore, the bandwidth factor is much less than unity for the HIBLEO-4 receivers.

$$B_f = 10\log_{10}(B_{sat} / B_{ANLE}) = -9.1 \quad \text{(dB)} \qquad (3\text{-}2)$$

Since adjacent-channel interference is ignored in the present analysis, we thus only need to consider the situation where, in each of the 497 towered airports, no more than two ANLE sectoral transmitters are transmitting at a given time into the victim passband.

4 Analysis Methodology and Results

This section presents the interference computation results based on the parameters discussed in Sections 2 and 3.

4.1 Baseline Calculations

The basic equation [13] for the received signal level (in dBm) at the satellite receiver from the i^{th} ANLE transmitter is as follows:

$$P_{r,sat}^{(i)} = P_t^{(i)} + (G_t^{(i)} - L_c) + G_r^{(i)} - L_{free}(d^{(i)}) - L_{feed} - L_p + B_f \quad (4\text{-}1)$$

where:

$P_t^{(i)}$ = i^{th} transmitter power (dBm)
$G_t^{(i)}$ = i^{th} transmitter antenna gain (dBi) toward satellite
L_c = cable/line loss
$G_r^{(i)}$ = satellite antenna gain (dBi) toward the i^{th} transmitter
L_{free} = free-space path loss (dB)
L_{feed} = feed loss (dB)
L_p = polarization discrimination (dB)
B_f = bandwidth factor (dB)
$d^{(i)}$ = distance (km) between i^{th} ANLE transmitter and satellite receiver.

The total received power from all N_v ANLE transmitters in view of the satellite receiver, expressed in dBW, is obtained as:

$$P_{r,sat}(\text{dBW}) = 10\log_{10}\left(\sum_{i=1}^{N_v} 10^{\frac{P_{r,sat}^{(i)}(\text{dBm})-30}{10}}\right) \quad (4\text{-}2)$$

For any given analysis scenario, the aggregate interference power attains a maximum value for a certain subsatellite point (the "hot point"). On the basis of the assumed ANLE transmitter power (22.3 dBm for FL and 20.9 dBm for RL), the hot points associated with all ANLE scenarios are determined (to 2° accuracy in latitude and longitude) from the interference power computation results at the relevant cells. The aggregate interference power reduction required to eliminate the interference, if applicable, can thus be determined from the difference between the hot point's interference power level and the interference threshold value.

4.2 Aggregate FL Interference Results for Various Scenarios

Our first investigations involved activating 1 to 2 BS sectors for FL transmission. Seven analyzed FL scenarios are categorized in Table 4-1.

Table 4-1. Characteristics for ANLE Scenarios with FL Transmissions

Scenario	Center Frequency (MHz)	ANLE Link Considered	Directions of Base Stations Main Beam
Scenario 1	5110	FL	BS_1 (0º) and BS_2 (240º)
Scenario 2	5120	FL	BS_1 (120º) and BS_2 (0º)
Scenario 3	5100	FL	BS_1 (240º) and BS_3 (0º)
Scenario 4	5130	FL	BS_2 (120º) and BS_3 (240º)
Scenario 5	5140	FL	BS_3 (120º)
Scenario 6	5100	FL	BS_1 (230º) and BS_3 (350º)
Scenario 7	5100	FL	BS_1 (240º+δ°) and BS_3 (100º+δ°)*

*Angle δ is constant for any given airport, but randomly selected from airport to airport.

Results for scenarios 1 to 6 can be found in Appendix A. It is seen that all results are below the interference threshold for these scenarios. Among Scenarios 1 to 5, Scenario 3 has the largest aggregate interference power at the hot point of -158.3 dBW. The hot point location is at (67° N, 114° W). The results for Scenario 3 are shown in Figure 4-1.

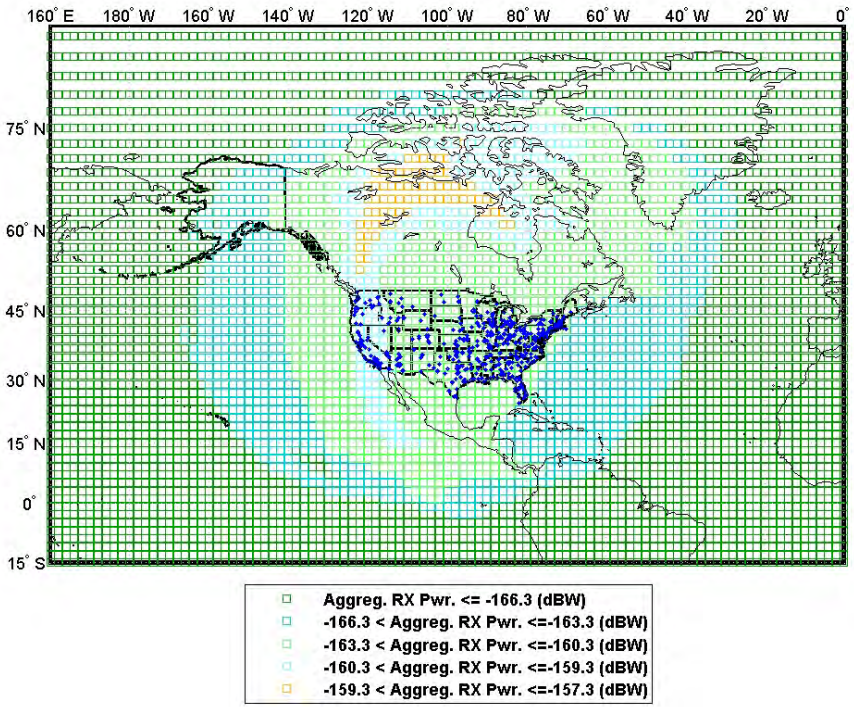

Figure 4-1. Aggregate RX Power from ANLE Transmissions in Scenario 3

Additional scenarios were run using the center frequency and geometry configuration of Scenario 3, but with different azimuth angles. The largest aggregate interference power at the hot point for any of the additional scenarios was -158.2 dBW, very close to the -158.3 dBW value observed for Scenario 3. This scenario was denoted as Scenario 6, whose results can be seen in Appendix A.

For the first six scenarios described above, it is assumed that the ANLE networks at all airports have the same directions for the base station sectors. While such situations can occur, it is more likely that while the ANLE configuration within an airport is maintained the same, the relative orientations among the airports would vary. Such a variation is expected to reduce the aggregate receive power from ANLE transmissions due to the variations in the sectoral antenna gains in azimuth (i.e., the antenna gain is smaller for azimuth angles different from the main beam direction). Scenario 7 modeled this effect by using various relative orientations described by the angle δ (which has different randomly selected values for different airports).

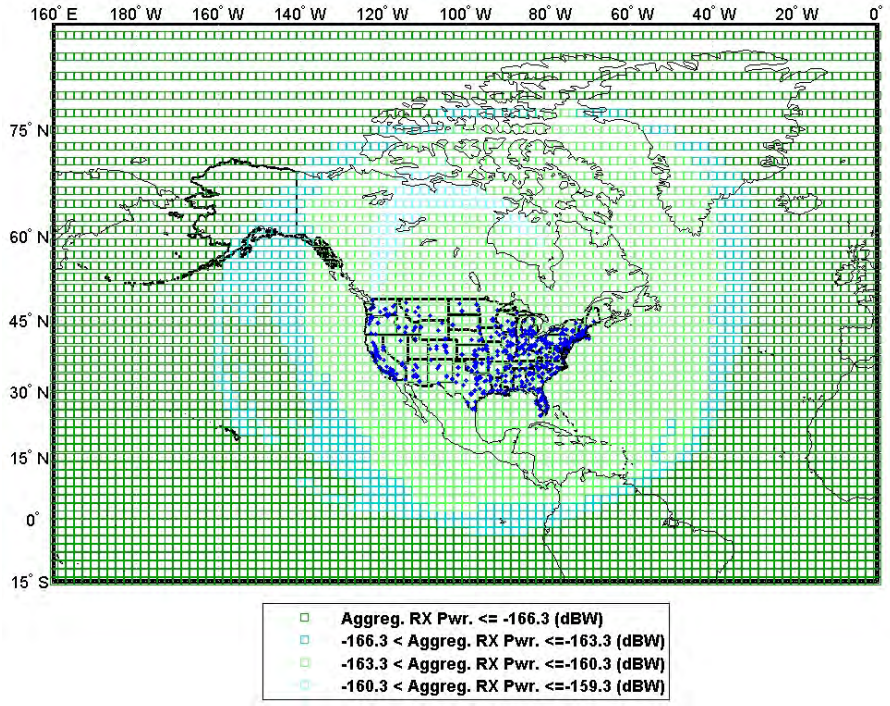

Figure 4-2. Aggregate RX Power from ANLE Transmissions in Scenario 7

As expected, the aggregate power at the satellite receiver is reduced, as can be seen by comparing the results in Figure 4-2 with the results in Figure 4-1.

4.3 Multiple OFDMA Transmissions

As discussed in [1] and [2], in OFDMA, the data subcarriers are divided into subsets, each of which is identified as a subchannel. This allows for simultaneous transmissions by multiple users (i.e., multiple subscriber units) to a given base station on the reverse link (RL); each user might be allocated one or more subchannels.

To evaluate the aggregate interference at the satellite receiver from multiple subscriber units that are transmitting to a given base station sector denoted as BS_{kl} (i.e., on the RL), and are

located within an airport area (denoted as a circle of radius R_0), the following observations can be made regarding the geometry of the problem shown in Figure 3-1:

$$2R_0 << h \text{ (6 km compared to 1414 km)} \quad (4\text{-}3)$$

and therefore

$$2r_0 << h \text{ (3.46 km compared to 1414 km)} \quad (4\text{-}4)$$

This means that, for any subscriber units denoted as *m*, *n*, the following expressions can be obtained for their antenna gains:

$$G_{SU}(\xi_{SU_{m,kl},sat}) \cong G_{SU}(\xi_{SU_{n,kl},sat}) \quad (4\text{-}5)$$

with the elevation angles from subscriber units to the satellite location are denoted as ξ.

These subscriber units are located within the circle of radius R_0 and served by a given BS sector denoted as BS_{kl} in any airport where an ANLE network is implemented. (For example, using this notation, the sector from BS_1 oriented with an azimuth angle of 0° would be denoted as BS_{11}.)

Using the observations regarding the geometry of the problem, the following expressions can be obtained for the various distance ratios:

$$\left| \frac{d_{SU_{n,kl},sat} - d_{SU_{m,kl},sat}}{d_{SU_{m,kl},sat}} \right| << 1 \quad (4\text{-}6)$$

The power received at a satellite location from a subscriber unit served by BS_{kl} can be expressed as:

$$P_{r,sat}^{(SU)(m,kl)} = P_{SU_{m,kl}}^{(RL)} + G_{SU}(\xi_{SU_{m,kl},sat}) + F_{SU_{m,kl}}^{(sat)} \quad (4\text{-}7)$$

where:

$$F_{SU_{m,kl}}^{(sat)} = G_{sat} + B_f - L_{total}(d_{SU_{m,kl},sat}) \quad (4\text{-}8)$$

is a factor that denotes the gains, and all the losses along the path from SU_m served by BS_{kl} to the satellite location, and:

$$B_f = \min(10\log_{10}(B_{sat} / B_{ANLE}), 0)$$

The equation for the $F_{SU}^{(sat)}$ factor takes into account the fact that the satellite antenna gain is assumed constant in the field of view as described in Section 3; therefore it does not depend on the off-axis angle between the SU location and the satellite location.

Using the observations discussed above, it can be shown that

$$F_{SU_{m,kl}}^{(sat)} \cong F_{SU_{n,kl}}^{(sat)} \cong F_{SU_{(kl)}}^{(sat)} \quad (4\text{-}9)$$

for any subscriber unit in the coverage area of the BS_{kl}.

In order to evaluate the uplink RFI from ANLE RL transmissions, power levels from all users (i.e., subscriber units) that are transmitting simultaneously at a given airport need to be taken into account. The following additional assumptions are used:

- Each user can be allocated one or more subchannels by the base station sector.
- Power control is implemented on the reverse link as described in the standard documents [1], [2], and [14].

The aggregate interference power received at the satellite from *all* subscriber units in the coverage area of BS_{kl} (assumed transmitting on all subchannels on the RL) can be described as:

$$P_{r,agg,SU_{(kl)}}^{(sat)} \leq P_{SU}^{(RL)} + G_{SU}(\xi_{SU_{(kl)},sat}) + F_{SU_{(kl)}}^{(sat)} \qquad (4\text{-}10)$$

The derivation of the above formula is discussed in Appendix B. The upper bound (identified by the equality condition above) can be obtained, for example, for a scenario where a given SU located at the edge of the coverage area of a given base station sector BS_{kl} is provided all subchannels on the reverse link, and therefore it transmits at the maximum power $P_{SU}^{(RL)} = P_{SU}$ =20.9 dBm.

4.4 Aggregate Interference Results on the RL

Scenarios using subscriber units transmitting at maximum power on the reverse link are analyzed in this section. Therefore, as discussed in the previous section, these are worst-case scenarios in terms of the aggregate power from the ANLE transmissions on the reverse link.

As presented in Figure 2-1, the configuration analyzed for ANLE networks uses three base stations, each with three sectors. Two different base station sectors can use the same frequency channel. Therefore, in analyzing worst-case potential interference to satellite receivers from ANLE RL transmissions, two different maximum power transmissions could occur from SUs served by two different base station sectors using the same frequency channel. These two subscriber units can be located very close to each other, or very far apart. Two different RL scenarios are analyzed, one with the farthest 2 SU locations, and one with the closest two SU locations. The geometry of these SU locations is illustrated in Figure 4-3. The derivation of this geometry is discussed in Appendix B.

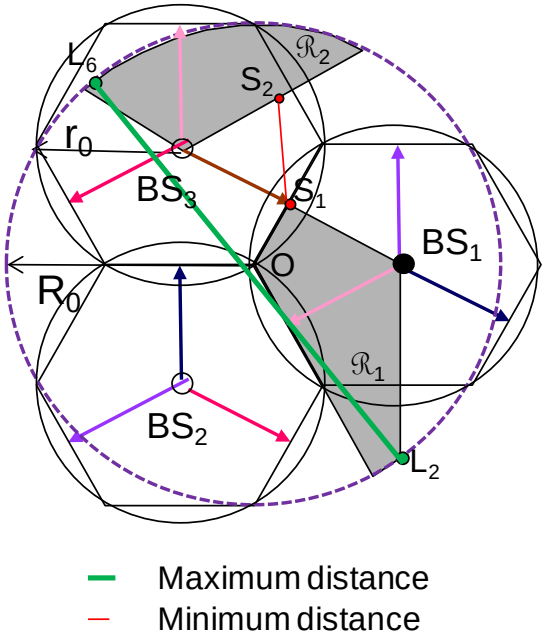

Figure 4-3. Subscriber Unit Locations for RL Transmissions

The first RL scenario uses two subscriber units located at the maximum distance from each other (with their locations denoted as L_2 and L_6 in Figure 4-3) in each airport that uses an ANLE network. Each one of these SUs transmits at maximum power. Thus, from an aggregate power transmitted on the RL by ANLE networks, this is a worst-case scenario. This scenario is denoted as Scenario 8.

The second RL scenario uses two subscriber units located at minimum distance from each other (with their locations denoted as S_1 and S_2 in Figure 4-3) in each airport that uses an ANLE network. Again, each one of these SUs transmits at maximum power, so in terms of an aggregate power transmitted on the RL by ANLE networks this is also a worst-case scenario, but with a different geometry from that of the first RL scenario. This scenario is denoted as Scenario 9.

Table 4-2. Characteristics for ANLE Scenarios with RL Transmissions

Scenario	Center Frequency (MHz)	ANLE Link Considered	Subscriber Units Locations
Scenario 8	5100	RL	L_2 and L_6
Scenario 9	5100	RL	S_1 and S_2

The results from Scenario 8 are shown in Figure 4-4. Comparing the results from Figure 4-1 (or 4-2) and Figure 4-4, it can be seen that RL ANLE transmissions generate lower aggregate power levels at the satellite receiver locations than the FL ANLE transmissions.

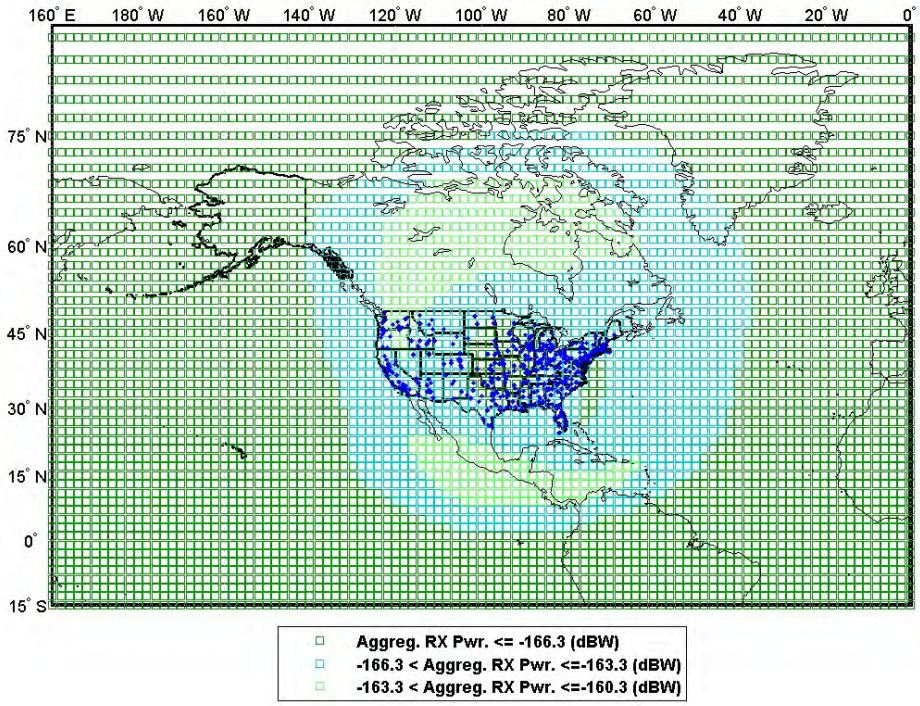

Figure 4-4. Aggregate RX Power from ANLE Transmissions in Scenario 8

Results from Scenario 9 are very similar to those from Scenario 8, and are shown in Appendix A. This is expected, due to the geometry of the problem described by equation (4-3) and the fact that the subscriber unit antennas are omnidirectional (i.e., there is no azimuth variation in the SU antenna gains).

For each scenario, the satellite location where the aggregate received power level from ANLE transmissions reaches its maximum is denoted as the "hot point" for that scenario. The hot point locations and the aggregate powers are shown in Table 4-3 for each of the nine scenarios discussed above. As the table shows, for each scenario, the maximum aggregate received power at the satellite from ANLE transmissions is below the interference threshold of -157.3 dBW.

Table 4-3. Aggregate Received Powers from ANLE Networks

Scenario Class	Scenario	"Hot Point" Location	Aggregate Received Power (dBW) at Hot Point	ANLE-to-MSS Interference Margin (dB)
FL with standard sectoral azimuths at all airports	1	(67°N, 114°W)	-158.3	1.0
	2	(67°N, 108°W)	-158.5	1.2
	3	(67°N, 114°W)	-158.3	1.0
	4	(11°N, 90°W)	-159.2	1.9
	5	(15°N, 64°W)	-161.0	3.8
	6	(67°N, 114°W)	-158.2	0.9
FL with randomized azimuths	7	(67°N, 114°W)	-159.5	2.2
RL	8	(65°N, 96°W)	-161.9	4.6
	9	(65°N, 96°W)	-161.9	4.6

As discussed above, in all the scenarios analyzed (with ANLE transmissions on the FL and RL), the aggregate RFI power levels are seen to be below the threshold value. In addition, the ITU-R M.1827 recommendation identified a maximum power flux density (pfd) PFD_{max} of -145.77 dBW/(m^2x1.23 MHz) at the satellite receiver produced by one AM(R)S transmitter (i.e., ANLE transmitter). For the analyzed scenarios, this maximum pfd level is also met. Using the methodology discussed in ITU-R M.1827, we have also considered a maximum aggregate pfd value at the satellite receiver antenna from all ANLE transmitters that would be -121.79 dBW/(m^2x1.23 MHz). We meet this aggregate limit as well for the analyzed scenarios.

Therefore, using the findings described above, RFI mitigation methods are not needed for any of the scenarios evaluated in this study, given the parameters and assumptions on which our analysis was based.

Although no mitigation is needed for the given set of parameters and assumptions, if a reduction in the aggregate received power from ANLE transmissions at the satellite receiver is desired, the following methods could be further investigated for potential implementation: utilization of receivers with better sensitivities, use of base station antennas with lower side lobes, use of practical ANLE duty-cycle values (i.e., below 100%), and/or use of additional frequency channels.

5 Concluding Remarks

Based on the results of this analysis, it seems feasible for ANLE systems using the OFDMA implementation of the IEEE 802.16e standard to share the 5091-5150 MHz band with non-GSO MSS feeder uplinks for HIBLEO-4 satellites, provided that:

- The 2% interference criterion applies, and
- The assumptions and parameters for ANLE networks and MSS satellites identified in this study are applied.

For this analysis we used a number of assumed values for various margins in an ANLE system. These values should be further validated by simulations and/or field tests (which are beyond the scope of the present study).

It should be noted that the new RTCA special committee (SC) 223 on Airport Surface Wireless Communications [15] is developing aviation system profiles for wireless broadband networks in the airport environment, which are denoted as ANLE networks in this report. As these aviation profiles are developed, and the characteristics of these networks evolve, the ANLE/MSS compatibility analysis should be updated as needed to reflect the new findings.

6 List of References

1. IEEE, February 2006, *IEEE Standard for Local and Metropolitan Area Networks, Part 16: Air Interface for Fixed and Mobile Broadband Wireless Access Systems, Amendment 2: Physical and Medium Access Control Layers for Combined Fixed and Mobile Operation in Licensed Bands and Corrigendum 1*, IEEE Std 802.16e-2005.
2. IEEE, October 1, 2004, *IEEE Standard for Local and Metropolitan Area Networks, Part 16: Air Interface for Fixed Broadband Wireless Access Systems*, IEEE Std 802.16-2004.
3. Hoh, Y., I. Gheorghisor, and F. Box, March 2005, *Feasibility Analysis of 5091-5150 MHz Band Sharing by ANLE and MSS Feeder Links*, MITRE Paper (MP) 05W0000083, The MITRE Corporation, McLean, VA.
4. Gheorghisor, I., A. Leu, and W. Wilson, September 2009, *Modeling of ANLE Networks*, MITRE Technical Report (MTR) 090296, The MITRE Corporation, McLean, VA.
5. Matolak, D. W., I. Sen, and W. Xiong, July 2008, "The 5-GHz Airport Surface Area Channel –Part I: Measurement and Modeling Results for Large Airports", *IEEE Trans. on Vehicular Technology*, Vol. 57, No. 4.
6. ITU-R F.1336-2, 2007, *Reference Radiation Patterns of Omnidirectional, Sectoral and Other Antennas in Point-to-Multipoint Systems for Use in Sharing Studies in the Frequency Range from 1 GHz to above 70 GHz.*
7. WiMAX Forum, July 2008, *WiMAX System Evaluation Methodology*.
8. ITU-R, January 10, 2007, *Additional Technical Details Supporting IP-OFDMA as an IMT-2000 Terrestrial Radio Interface*, ITU Question ITU-R 229-1/8.
9. IEEE, 29 May 2009, *IEEE Standard for Local and Metropolitan Area Networks, Part 16: Air Interface for Broadband Wireless Access Systems*, IEEE Std 802.16-2009.
10. WRC, *Final Acts WRC-07*, World Radiocommunication Conference, Geneva, 2007.
11. ITU-R, *Technical and operational requirements for stations of the aeronautical mobile (R) service (AM(R)S) limited to surface application at airports and for stations of the aeronautical mobile service (AMS) limited to aeronautical security (AS) applications in the 5091-5150 MHz*, ITU-R M.1827 (2007 version).
12. ITU-R, *e.i.r.p. Density Limit and Operational Restrictions for RLANs or Other Wireless Access Transmitters in Order to Ensure the Protection of Feeder Links of Non-Geostationary Systems in the Mobile-Satellite Service in the Frequency Band 5150-5250 MHz*, ITU-R M.1454 (2000 version).
13. Gheorghisor, I., Y. Hoh, and F. Box, October 15, 2006, "5091-5150 MHz Bandsharing by Airport Wireless Local Area Networks and Satellite Feeder Links", *IEEE DASC*.
14. Eklund, Carl, et al., 2006, *WirelessMAN Inside the IEEE 802.16 Standard for Wireless Metropolitan Networks*, Standards Information Network, IEEE Press, New York, NY.

15. RTCA, 2009, SC-223 Airport Surface Wireless Communications, http://www.rtca.org/comm/Committee.cfm?id=133
16. Gheorghisor, I., July 2008, *Spectral Requirements of ANLE Networks for the Airport Surface*, MP080109R1, The MITRE Corporation, McLean, VA.

Appendix A Additional Aggregate Power Results

The following figures illustrate the aggregate power computation results from ANLE transmissions on the forward link. Although the aggregate interference power levels are below the threshold value at all locations for all of these plots, the relative exposure of different satellite locations is clearly shown in each plot.

Scenarios 1 and 3 provide very similar results. This was expected, because the directions of the respective main beams are the same in the two BS sectors.

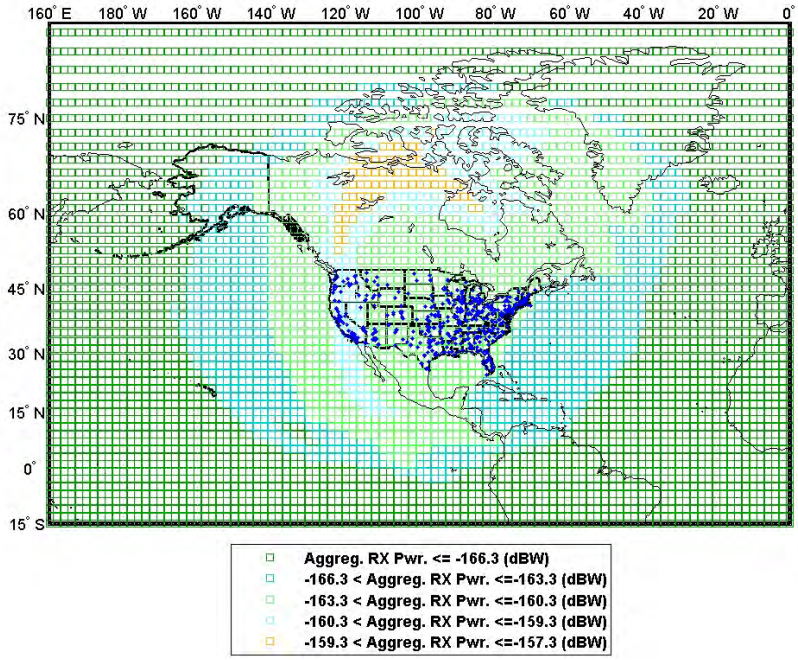

Figure A-1. Aggregate RX Power from ANLE Transmissions in Scenario 1

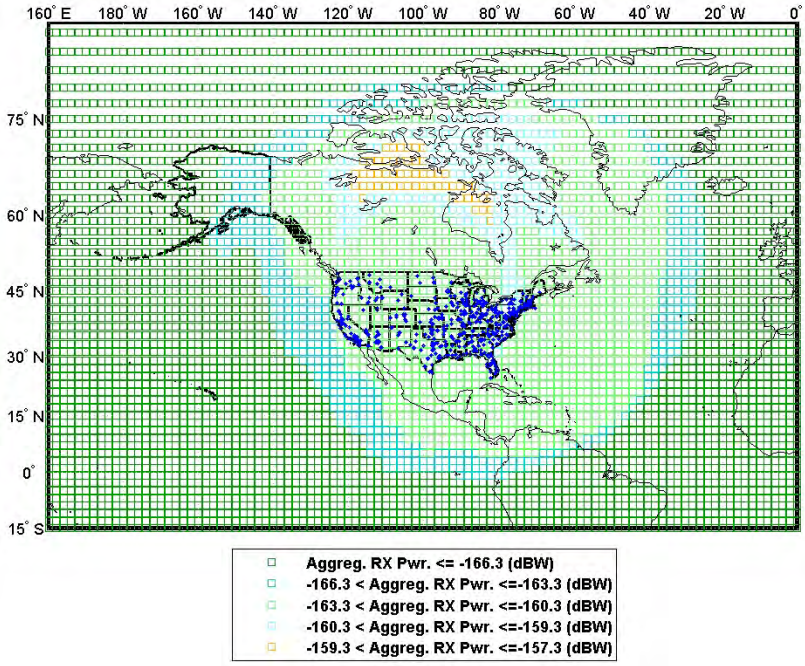

Figure A-2. Aggregate RX Power from ANLE Transmissions in Scenario 2

Among the first five scenarios, Scenario 3 provides the largest aggregate interference power (-158.3 dBW) at the hot point (67° N, 114° W) for this scenario.

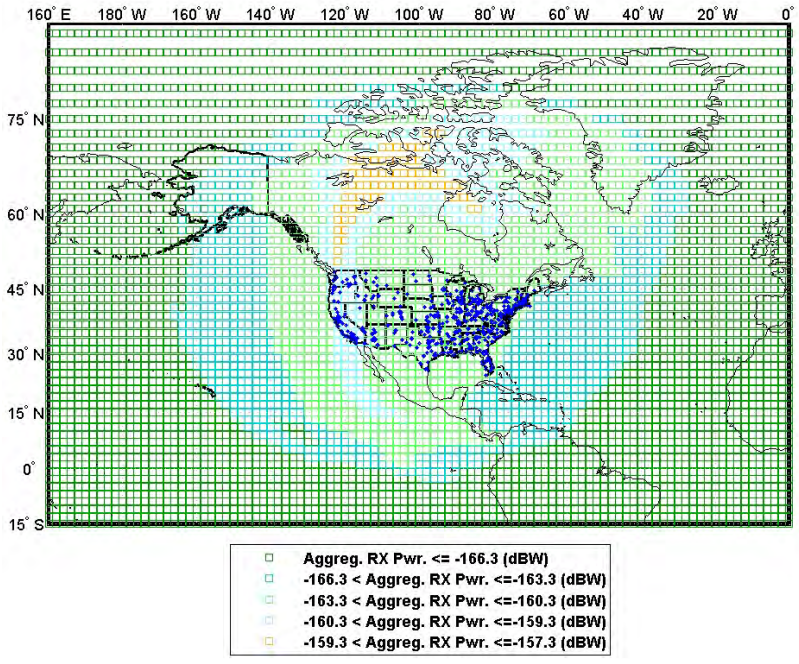

Figure A-3. Aggregate RX Power from ANLE Transmissions in Scenario 3

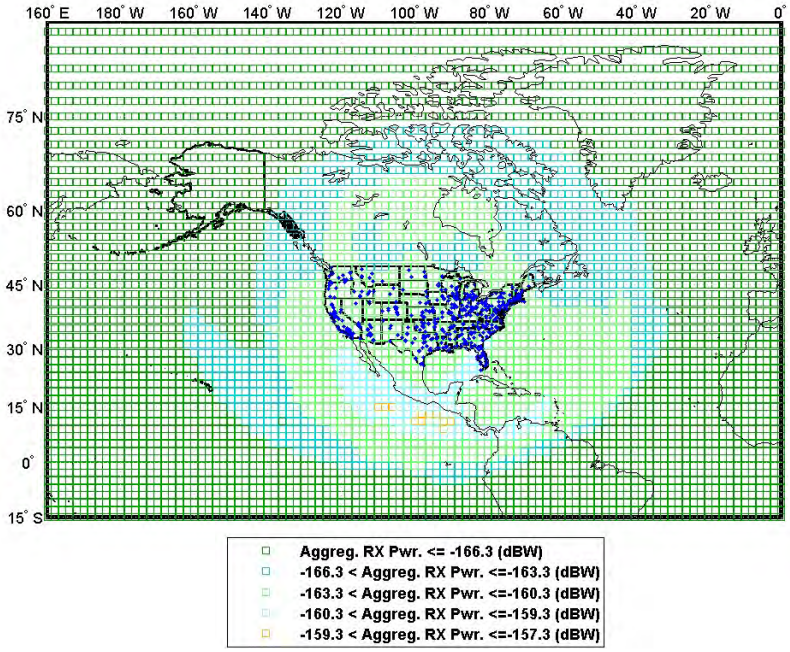

Figure A-4. Aggregate RX Power from ANLE Transmissions in Scenario 4

Scenario 5 provides the smallest amount of potential interference, since only one BS sector is transmitting at each airport.

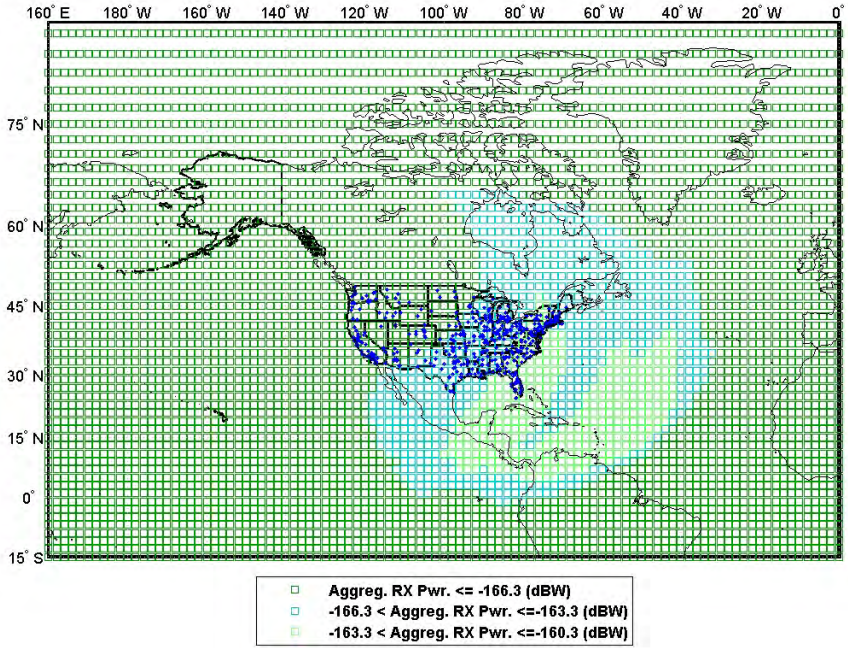

Figure A-5. Aggregate RX Power from ANLE Transmissions in Scenario 5

Results from Scenarios 6 are shown in Figure A-6. For this scenario the center frequency and the geometry are the same as for Scenario 3, but the azimuth angles of the main beams of the base station antennas are 230° for BS_1 and 350° for BS_3. The aggregate power level in this configuration is -158.2 dBW, as discussed in Section 4.2.

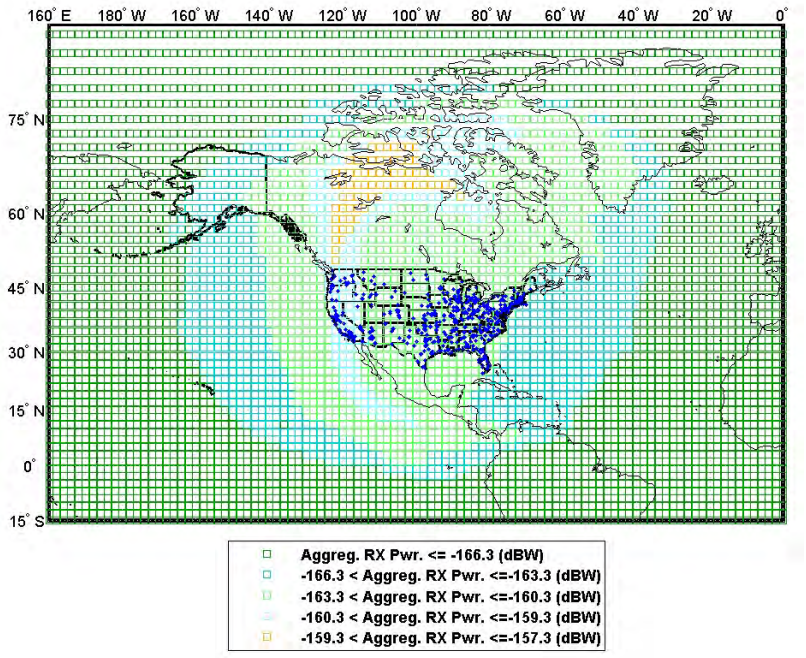

Figure A-6. Aggregate RX Power from ANLE Transmissions in Scenario 6

Results from Scenario 9 are shown in Figure A-7. As discussed in Section 4.2, these results are very similar to those from Scenario 8, and are shown here for completeness.

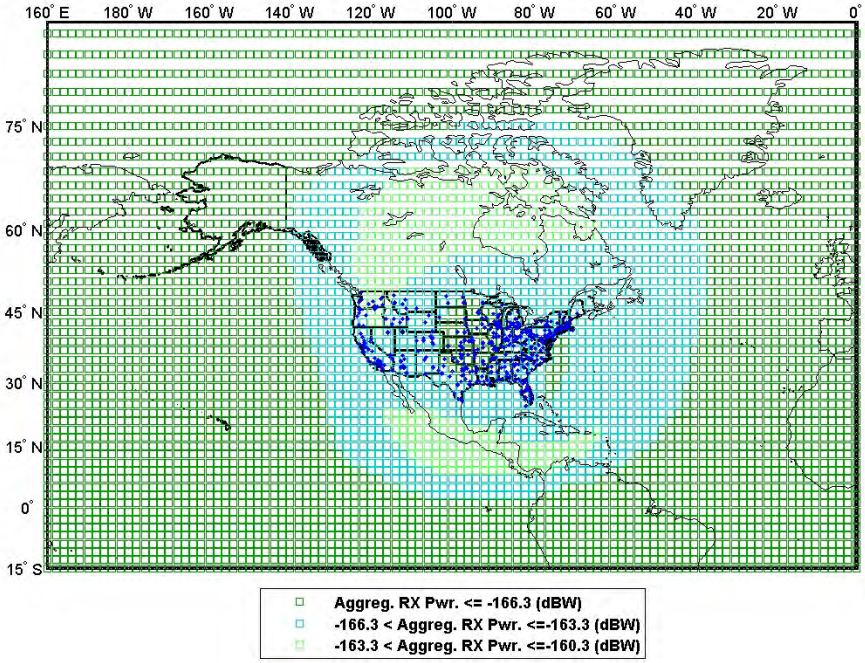

Figure A-7. Aggregate RX Power from ANLE Transmissions in Scenario 9

Appendix B Additional Derivations for ANLE RL Transmissions

B.1 Additional Derivation for Multiple OFDMA Transmissions

In order to evaluate the uplink RFI from ANLE RL transmissions, power levels from all users (i.e., subscriber units) that are transmitting simultaneously at a given airport need to be taken into account. The following additional assumptions are used:

- Each user can be allocated one or more subchannels by the base station sector.
- Power control is implemented on the reverse link as described in [1], [2], and [14].

The following equations can be identified for the RL analysis for any subscriber unit served by a given base station sector BS_{kl}. In this notation, the index *i* denotes the modulation and coding index as described in [16]. It is also assumed that one subchannel is assigned to a subscriber unit *p* with the modulation and coding index *i*.

$$P_{r,sch,BS_{kl}}^{(i)(RL)} = P_{t,sch,SU_p}^{(i)(RL)}(d) + G_{SU_p} - L_{path}(d) - L_{fm} - L_{im} + G_{rx,div} - L_{sm} + G_{BS_{kl}} - L_c \geq R_{xs,sch,BS}^{(i)(RL)} \quad \text{(B-1)}$$

with: $d_{i+1} \leq d \leq d_i$ for $i = 1...6$ and $d_{\min} \leq d \leq d_i$ for $i = 7$

where:

$$R_{xs,sch,BS}^{(i)(RL)} = R_{xs,sch,BS}^{(1)(RL)} + \Delta SNR(i)\ i = 1 \ldots 7 \quad \text{(B-2)}$$

$$R_{xs,sch,BS}^{(1)(RL)} = R_{xs,BS}^{(1)} - 10 * \log_{10}(N_{Tsch}^{(RL)}) \quad \text{(B-3)}$$

$R_{xs,BS}^{(1)}$ = -92.36 dBm as discussed in the Section 2.3

$N_{Tsch}^{(RL)}$ = number of RL subchannels (= 35 for BW = 10 MHz)

$R_{xs,sch,BS}^{(1)(RL)}$ is the composite receiver sensitivity at the BS for a subchannel (i.e., 24 subcarriers) on the RL for QPSK ½ modulation (i.e., modulation index 1)

It can be shown that:

$$P_{t,sch,SU_p}^{(i)(RL)}(d) = P_{t,sch,SU_p}^{(i)(RL)}(d_i) + 10n\log_{10}(d/d_i) \quad \text{(B-4)}$$

or, if the power values are presented as numeric, and denoted with subscript (num):

$$P_{t,sch,num,SU_p}^{(i)(RL)}(d) = P_{t,sch,num,SU_p}^{(i)(RL)}(d_i)\left(\frac{d}{d_i}\right)^n \quad \text{(B-5)}$$

with: $d_{i+1} \leq d \leq d_i$ for $i = 1...6$ and $d_{\min} \leq d \leq d_i$ for $i = 7$ (d_{min} = 15 m)

Therefore:

$$P_{t,sch,num,SU_p}^{(i)(RL)}(d) \le P_{t,sch,num,SU_p}^{(i)(RL)}(d_i)$$

for any distance d between d_{i+1} and d_i.

The distance parameters described above also have azimuth angle dependence because G_{BS} depends on the azimuth angle as described in the sectoral antenna pattern description in Section 2 for any BS sector denoted in analysis as BS_{kl}.

It can be shown that:

$$P_{t,sch,SU}^{(1)(RL)}(d_1) = P_{t,sch,SU}^{(i)(RL)}(d_i) \quad \text{for } i = 2...7 \tag{B-6}$$

where

$d_1(0)=r_0 = 1.73$ km for a subscriber unit at the edge of the coverage area of the given BS sector, in the main beam of the BS antenna (i.e., azimuth angle denoted as 0), and using the modulation and coding QPSK ½ (which is assumed as having the index 1). The azimuth angle dependence for the various distances is also shown in Figure B-1.

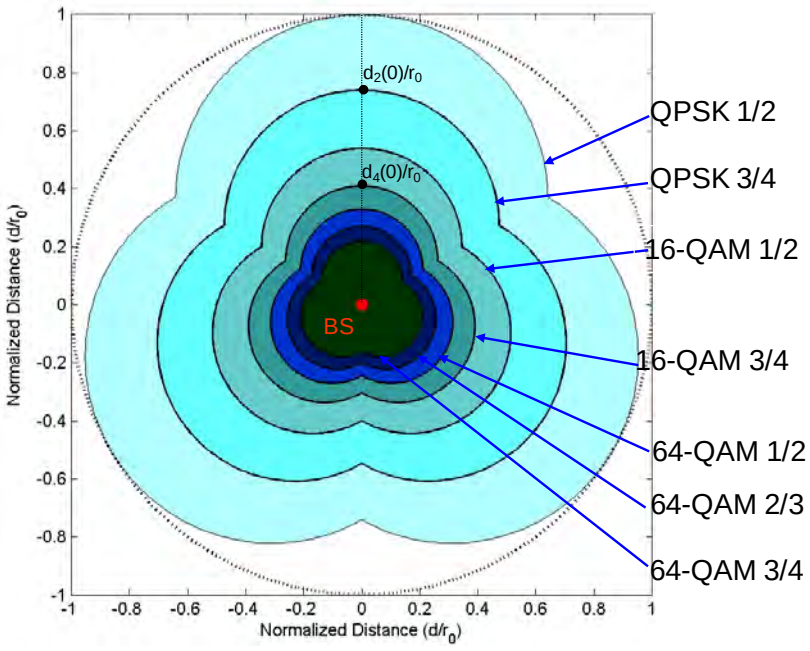

Figure B-1. Adaptive Modulation Illustration for a Sectorized Base Station

The upper bound of the received aggregate power at a given satellite location from all subscriber units that are transmitting to a given BS denoted as BS_{kl} (therefore from all subchannels on the RL) is evaluated below using all the results obtained above as well as the results of the geometry analysis presented in Section 4.

The received aggregate power is:

$$P_{r,agg,SU_{(k)},num}^{(sat)} \le N_{Tsch}^{(RL)} F_{SU_{(kl)},num}^{(sat)} G_{SU,num}(\xi_{SU_{(kl)},sat}) P_{t,sch,SU}^{(1)(RL)}(d_1) \tag{B-7}$$

Therefore the aggregate interference power received at the satellite from *all* subscriber units in the coverage area of BS_{kl} is:

$$P_{r,agg,SU_{(kl)}}^{(sat)} \le P_{SU}^{(RL)} + G_{SU}(\xi_{SU_{(kl)},sat}) + F_{SU_{(kl)}}^{(sat)} \qquad \text{(B-8)}$$

The upper bound (identified by the equality condition in the formula above) can be obtained, for example, for a scenario where a given SU located at the edge of the coverage area of a given base station sector BS_{kl} is provided all subchannels on the reverse link, and therefore it transmits at the maximum power $P_{SU}^{(RL)} = P_{SU} = 20.9$ dBm.

B.2 Derivations for Subscriber Unit Locations for ANLE RL Transmissions

B.2.1 Closest Locations for Subscriber Units

The closest locations where two subscriber units (SUs) transmit at the maximum allowable power are at the following coordinates: $S_1\left(r_0/4, r_0\sqrt{3}/4\right)$ and

$$S_2\left(-\frac{1-0.74\cdot\sqrt{3}}{2}r_0, \frac{0.74+\sqrt{3}}{2}r_0\right).$$

Proof: Let M_1 and M_2 two locations arbitrarily chosen within the regions $\Re_1$ and $\Re_3$, respectively. Also let S_1P be perpendicular to O_3A.

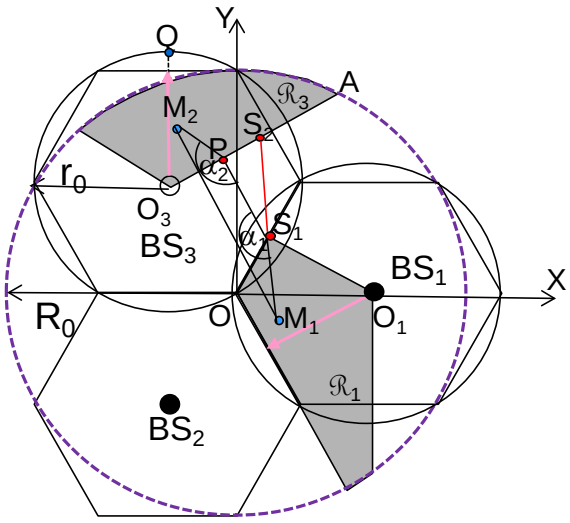

Figure B-2. The Closest Locations

Since the angles α_1 and α_2 are greater than 90^o for any M_1 and M_2, then $M_1M_2 \ge S_1P$.

The maximum power transmitted by an SU in location Q, denoted as P_{SU}, satisfies the following equation:

$$P_{SU} + G_{SU} - L_{other} - 23\log_{10}(r_0) + G_{BS_{31}}(0) = R_{xs,BS} \quad \text{(B-9)}$$

Now, considering the maximum transmit power constraint, we can observe that the locations separated with the distance that is closest to S_1P are S_1 and S_2, such that $O_3S_2 = l_2$, where l_2 is the distance from SU_2 to the BS_{31} that requires the transmit power $P_{SU,2}$ reaches the maximum level, P_{SU}. Mathematically, the transmit power of a SU located at S_2 is:

$$P_{SU,2} = R_{xs,BS} - G_{SU} + L_{other} + 23\log_{10}(l_2) - G_{BS_{31}}(\phi_2) \quad \text{(B-10)}$$

where l_2 and ϕ_2 are the distance and the azimuth angle of the location S_2 relative to base station sector BS_{31}.

From (B-9) and (B-10), we obtain:

$$P_{SU,2} - P_{SU} = G_{BS_{31}}(0) - G_{BS_{31}}(\phi_2) + 23\log_{10}(l_2 / r_0) \quad \text{(B-11)}$$

Hence, since $P_{SU,2} = P_{SU}$ and $\phi_2 = 60^o$ such that $G_{BS_{31}}(0) - G_{BS_{31}}(\phi_2) = 3\,\text{dB}$, we find that $l_2 = 0.74r_0$.

Considering O to be the origin (0,0), then the coordinates of these locations are $S_1\left(r_0/4, r_0\sqrt{3}/4\right)$ and $S_2\left(-\frac{1-0.74\cdot\sqrt{3}}{2}r_0, \frac{0.74+\sqrt{3}}{2}r_0\right)$.

B.2.2 Farthest Locations for Subscriber Units

The farthest two locations where two SUs transmit at the maximum allowable power are at the following coordinates: $L_2\left(r_0, -\sqrt{R_0^2 - r_0^2}\right)$ and $L_6(-1.96, 2.26)$.

Proof: We can notice that the maximum distance between the two locations from the two gray regions, $\Re_1$ and $\Re_3$, is $2R_0$. These two locations form a diameter of the circle of radius R_0 and centre O, such that one location between the points with the coordinates $L_1\left(R_0/2, -R_0\sqrt{3}/2\right)$ and $L_2\left(r_0, -\sqrt{R_0^2 - r_0^2}\right)$ and the second location between $L_3\left(R_0/2, R_0\sqrt{3}/2\right)$ and $L_4\left(r_0, -\sqrt{R_0^2 - r_0^2}\right)$.

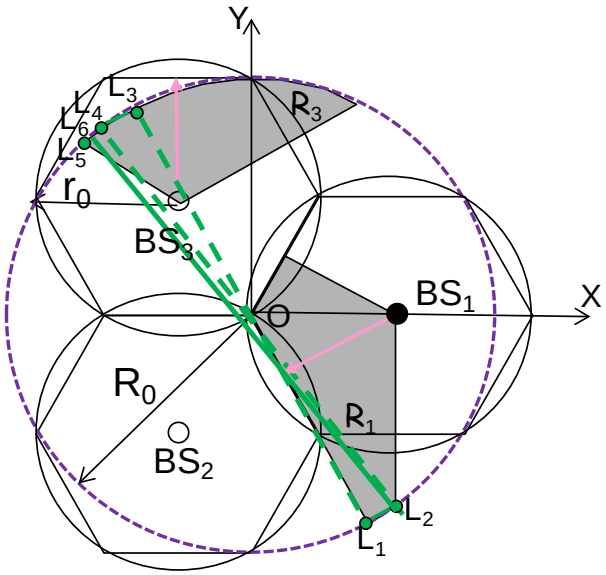

Figure B-3. Farthest Locations

Now, considering the maximum transmit power constraint, the transmit power required by the SU from the location on the circle with the radius R_0, between L_3 and L_4, is given by:

$$P_{SU}(l) + G_{SU} - L_{other} - 23\log_{10}(l) + G_{BS_{31}}(\phi) = R_{xs,BS} \quad \text{(B-12)}$$

where l is the distance between the SU and the BS_{31} sector, and ϕ is the azimuth angle from the main beam of the BS_{31} sector (shown in Figure B-3 with an arrow in region R_3), $R_{xs,BS}$ is the BS receiver sensitivity, and L_{other} describes all the other losses on the path between the SU and the BS sector.

As in equation (B-9), the maximum power transmitted by the SU, denoted as P_{SU}, is:

$$P_{SU} + G_{SU} - L_{other} - 23\log_{10}(r_0) + G_{BS_{31}}(0) = R_{xs,BS} \quad \text{(B-13)}$$

Let l_4 and ϕ_4 be the distance and the azimuth angle of the location L_4 relative to base station sector BS_{31}. The transmit power of a SU located at L_4 is:

$$P_{SU,4} = R_{xs,BS} - G_{SU} + L_{other} + 23\log_{10}(l_4) - G_{BS_{31}}(\phi_4) \quad \text{(B-14)}$$

Since $\phi_4 = -42^o$ and $l_4 = 1.2851$ km, we find that $P_{SU,4} < P_{SU}$, which shows there are no cases where SU locations within the circle of radius R_0 could be as far apart from each other as $2R_0$, because $P_{SU}(l) < P_{SU,4}$ for any location between L_3 and L_4.

In conclusion, the locations from which two SUs transmit at maximum power apart from each other with maximum distance are L_2 and L_6, such that L_6 is somewhere between L_4 and L_5. Therefore, the exact location, $L_6(x_6, y_6)$, is given by the following equation:

$$P_{SU} = R_{xs,BS} - G_{SU} + L_{other} + 23\log_{10}(l_6) - G_{BS_{31}}(\phi_6) \quad \text{(B-15)}$$

where $d_6 = \sqrt{x_6^2 + y_6^2}$ and ϕ_6 is the azimuth angle of the location L_6 relative to the base station sector BS_{31}.

From equations (B-13) and (B-15) we obtain the following expression:

$$23\log_{10}(l_6/r_0) = G_{BS_{31}}(\phi_6) - G_{BS_{31}}(0) \qquad \text{(B-16)}$$

The solution of equation (B-14), that can be determined graphically, provides the coordinates $x_6 \approx$ - 1.96 km and $y_6 \approx$ 2.26 km, and the azimuth angle $\phi_6 = -56°$.

Appendix C Glossary

AMS	Aeronautical mobile service
AMT	Aeronautical mobile telemetry
AM(R)S	Aeronautical mobile (route) service
ANLE	Airport Network and Location Equipment
AS	Aeronautical security
BS	Base station
CAASD	Center for Advanced Aviation System Development
CONUS	Contiguous United States
dB	Decibel
dBi	dB referred to lossless isotropic gain
dBm	dB referred to one milliwatt
dBW	dB referred to one watt
FAA	Federal Aviation Administration
FOV	Field of view
GHz	Gigahertz
IEEE	Institute of Electrical and Electronics Engineers
ITU	International Telecommunication Union
ITU-R	ITU Radio communication Sector
km	Kilometer
LAN	Local area network

LEO	Low-earth-orbit
MHz	Megahertz
MSS	Mobile-satellite service
Non-GSO	Non-geostationary
OFDM	Orthogonal Frequency-Division Multiplexing
OFDMA	Orthogonal Frequency-Division Multiple Access
pfd	Power flux density
QPSK	Quadrature Phase-Shift Keying
RF	Radio frequency
RFI	Radio frequency interference
SU	Subscriber Unit
WRC	World Radiocommunication Conference